The Blasius Function in the Complex Plane

John P. Boyd

CONTENTS

This work was supported by NSF grant OCE9521133.

The Blasius function, denoted by f, is the solution to a simple nonlinear boundary layer problem, a third order ordinary differential equation on $x \in [0, \infty]$. In this work, we calculate several numerical constants, such as the second derivative of f at the origin and the two parameters of the linear asymptotic approximation to f, to at least eleven digits. Although the Blasius function is unbounded, we nevertheless derive an expansion in rational Chebyshev functions TL_j which converges exponentially fast with the truncation, and tabulate enough coefficients to compute f and its derivatives to about nine decimal places for all positive real x. The power series of f has a finite radius of convergence, but the Euler-accelerated expansion is apparently convergent for all real x. We show that the singularities, which are first order poles to lowest order, have an infinite series of cosine-of-a-logarithm corrections. Lastly, we chart the behavior of f in the complex plane and conjecture that all singularities lie within three narrow sectors.

1. INTRODUCTION

The Blasius function is defined as the unique solution to the boundary value problem

$$2f_{xxx} + f f_{xx} = 0$$

subject to the boundary conditions

$$f(0) = f_x(0) = 0, \quad f_x(\infty) = 1.$$

Blasius himself [1908] derived both power series and asymptotic expansions and patched them together at finite x to obtain an approximation which agrees quite satisfactorily with later treatments. Why, then, have there been so many students of this problem as but partially catalogued in Table 1, including such luminaries as Hermann Weyl (three papers) and John von Neumann?

Part of the answer is the sheer challenge: the differential equation is so simple, the Blasius function so smooth (indeed monotonic) that it appears that it *must* have a simple analytic representation, or at

Reference	Comments
[Blasius 1908]	Matched power series to asymptotic solution
[Töpfer 1912]	Showed that boundary-value problem could be reduced, through group invariance, to a single integration of an initial-value problem; Runge–Kutta computation of $f_{xx}(0)$ to several digits
[Bairstow 1925]	Introduced $f_{xx} = \exp(-F/2)$ with $F \equiv \int_0 x f(y)\,dy$ and then approximated f in the integral by power series
[Piercy and Preston 1936]	Solved by successive approximations; computed $f_{xx}(0)$ with about 3% error
[Weyl 1941; 1942a; 1942b]	Converted ODE to integral equation which he solved by provably convergent iteration; showed that power series had radius of convergence ρ but bounds on ρ differed by more than 1.5
von Neumann (1941)	Showed that symmetries allowed reduction to a first order equation (unpublished, quoted by Weyl)
[Ostrowski 1948]	narrowed radius of convergence uncertainty
[Meksyn 1956]	
[Punnis 1956a]	narrowed convergence limits to $\pm 1/300$
[Punnis 1956b]	Showed numerically f has pole like $6/(x - x_s)$
[Meksyn 1959]	Showed that pole on the negative real axis is a trio of singularities at the same distance from $x = 0$
[Squire 1959a]	Applies generalized Gauss–Laguerre quadrature
[Squire 1959b]	Three-point boundary conditions
[Meksyn 1961]	
[Treve 1967]	Same boundary-value problem but very different boundary condition for electrical engineering problem

TABLE 1. Highlights in the history of the Blasius equation.

least simple, accurate approximations. Another motive is that the Blasius problem is the simplest of all nonlinear boundary layer problems. The hope has been that mathematical technologies developed for this epitome can then be applied to more difficult hydrodynamics problems.

In this article, we explore the Blasius function from a variety of perspectives. Our multiple lines of attack have affinities with the philosophy and sometimes the methodology of the work of Van Dyke, Hunter and others on computer-extended series [Van Dyke 1974; 1975a; 1975b; 1977; 1978; 1984; 1990; Meiron et al. 1982; Hunter and Lee 1986; Hunter and Tajdari 1990; Drazin and Tourigny 1996]. While we have been no more successful than others at deriving a simple analytic solution, we at least can explain why this seemingly well-behaved function is fraught with complications and perils.

2. CONTINUOUS SYMMETRIES AND TWO SPECIAL SOLUTION FAMILIES

The Blasius differential equation has two continuous symmetries. First, because the coefficients of the differential equation are independent of x, the solution is translationally invariant; that is, if $g(x)$ is a solution, then so is

$$f(x) \equiv g(x - \mu), \quad \text{with } \mu \text{ an arbitrary constant.}$$

Second, there is a "dilational" symmetry: if $g(x)$ is a solution, then so also is

$$f(x) \equiv \lambda g(\lambda x)$$

Töpfer [1912] observed that one could solve the Blasius problem by (i) performing a single initial value integration with $f_{xx}(0) = 1$ (or any other arbitrary value), (ii) evaluating the limit of f_x for large x, and then (iii) applying the dilational symmetry to rescale the solution so that the boundary condition at infinity is satisfied.

Two special solutions illustrate these symmetries. First, there is the two-parameter family of solutions which are linear polynomials in x:

$$f_{\text{linear}} \equiv \beta + \gamma x,$$

where β and γ are arbitrary complex constants. This family represents only a single *shape*; by applying the two continuous symmetries, one can generate any member of this family from a single member of the family, such as $f_{\text{linear}}(x; \beta = 1, \gamma = 1)$.

Second, there is the simple pole

$$f_{\text{pole}} \equiv \frac{6}{x - \mu}.$$

In this one-parameter family of solutions, the parameter is the location of the pole μ. This singular solution is invariant under the dilational symmetry, so the family is not expanded by applying dilations.

The general solution to the Blasius equation is a three-parameter family where the parameters are the complex-valued constants that are the initial conditions. However, the general solution contains only a one-parameter family of shapes in the sense that one can generate all the solutions by translating and dilating the one-parameter family of distinct shapes. The particular shape which is the Blasius function is, alas, not as simple as either a linear polynomial or a simple pole. These special solutions are nevertheless important because the Blasius function is *asymptotic* to both in different portions of the complex x-plane.

3. POWER SERIES AND ASYMPTOTIC SERIES

The power series begins

$$f(x) \approx \tfrac{1}{2}\kappa x^2 - \tfrac{1}{240}\kappa^2 x^5 + \tfrac{11}{161280}\kappa^3 x^8 - \tfrac{5}{4257792}\kappa^4 x^{11} + \cdots,$$

where $\kappa \equiv f_{xx}(0)$ is the curvature of the function at the origin. By integrating the initial value problem using 27 decimal place accuracy with 50,000 grid points and order-four Runge–Kutta time-marching, we determined

$$\kappa \approx 0.33205733621519630,$$

where all sixteen decimal places are believed correct.

One remarkable feature is that only every third power appears in the series. Thus, the curvature f_{xx} is a function of x^3 and is invariant under rotations by 120 degrees about the origin in the complex plane — it is C_3-invariant, to use the jargon of group theory. $|f|$ has an even higher degree of symmetry if the branch cuts are drawn symmetrically as explained in Section 10 below.

The alternation of signs suggests that convergence is limited by a singularity on the negative x axis. Through a procedure described later, we found that the singularity was at $x_s = -S$, where

$$S = 5.6900380545. \qquad (3–1)$$

Punnis [1956b] showed the existence of this pole, proved that its residue is exactly 6 and computed its approximate location. The C_3 symmetry in the complex x-plane implies that there must also be poles at $x = S\exp(\pm i\pi/3)$. However, near the pole, there is also an infinite series of logarithmic corrections (Section 8): the convergence-limiting singularity is both a pole and a branch point.

Blasius noted that

$$f \sim x + B \quad \text{as } x \to \infty,$$

where B is an as yet unknown constant. Substituting this into the differential equation — for f only and not for its derivatives — gives a *linear* differential equation for f_{xx}:

$$f_{xxx} + \tfrac{1}{2}(x + B)\, f_{xx} \sim 0 \quad \text{for } x \gg 1.$$

The general solution is

$$f_{xx} = Q\exp\bigl\{-\tfrac{1}{4}x(x + 2B)\bigr\}, \qquad (3–2)$$

where by high precision Maple calculations

$$\begin{aligned} Q &= 0.233727621285063, \\ B &= -1.720787657520503. \end{aligned} \qquad (3–3)$$

Blasius then solved his boundary value problem and determined the missing initial condition, $f_{xx}(0) = \kappa$, by patching the power series to the asymptotic approximation at some finite x.

Weyl [1941; 1942a; 1942b] strongly criticized Blasius because the asymptotic series diverges and the power series has but a finite radius of convergence. The theoretical minimum error in Blasius' patching is the error of the asymptotic approximation at $x = S$. However, this is only 1 part in 5800 for the second derivative. Even at $x \approx 3.345$ $(= S/2)$, where each term in the power series is approximately half its predecessor, the relative error in the approximation of f_{xx} by Equation (3–2) is only 2.3%. So, Weyl's objection is not compelling unless one wants high accuracy. His objection is completely removed by the refinement explained in the next section.

4. EULER ACCELERATION OF THE POWER SERIES

The Euler method is an ancient scheme for transforming a slowly convergent or divergent power series into a more rapidly convergent series by making a change of coordinate. The Blasius function is an interesting application of Euler acceleration for the following reasons. First, the usual change of coordinate must be modified to respect the C_3 symmetry of the Blasius function. Second, the Eulerized series provides useful and hitherto unavailable information about singularity-free regions in the complex x-plane. Third, the Eulerized series appears to converge everywhere on the positive real x-axis. Thus, Blasius' procedure of patching power-series-to-asymptotic-series is capable of arbitrary accuracy, destroying Weyl's objection. A Taylor series is a very powerful tool when combined with enhancements such as Euler acceleration.

The fundamental idea, from [Van Dyke 1975b], is to make a change of coordinate so as to map the convergence-limiting singularity, here at $x = -S$, to infinity in a new coordinate ζ while simultaneously choosing the form of $\zeta(x)$ so that the first N terms of the power series in x are all that is needed to compute the first N terms of the power series in ζ. The special challenge of the Blasius function is that there are actually *three* convergence-limiting singularities. We can move all three to infinity by replacing x by x^3 in the usual transformation:

$$\zeta \equiv \frac{2x^3}{S^3 + x^3} \;\leftrightarrow\; x^3 = S^3 \, \frac{\zeta}{2 - \zeta}.$$

The denominator vanishes so that $\zeta = \infty$ when $x = S \exp(i(2j+1)\pi/3$, for $j = 0, 1, 2$, so that all three convergence-limiting singularities are indeed mapped away. However, the mapping itself is singular at $\zeta = 2$, which is mapped to $x = \infty$, so the radius of convergence in ζ will not be larger than 2 unless f is regular at infinity. This is not the case here since $f \to \infty$ as $x \to \infty$. The radius of convergence in ζ may be less than 2 if f has additional singularities which map to $|\zeta| < 2$, so the Eulerized series gives information about the distribution of singularities of $f(x)$.

Write the power series for f as

$$f(y) = y^2 \sum_{j=1}^{\infty} a_j \, y^{3j-3},$$

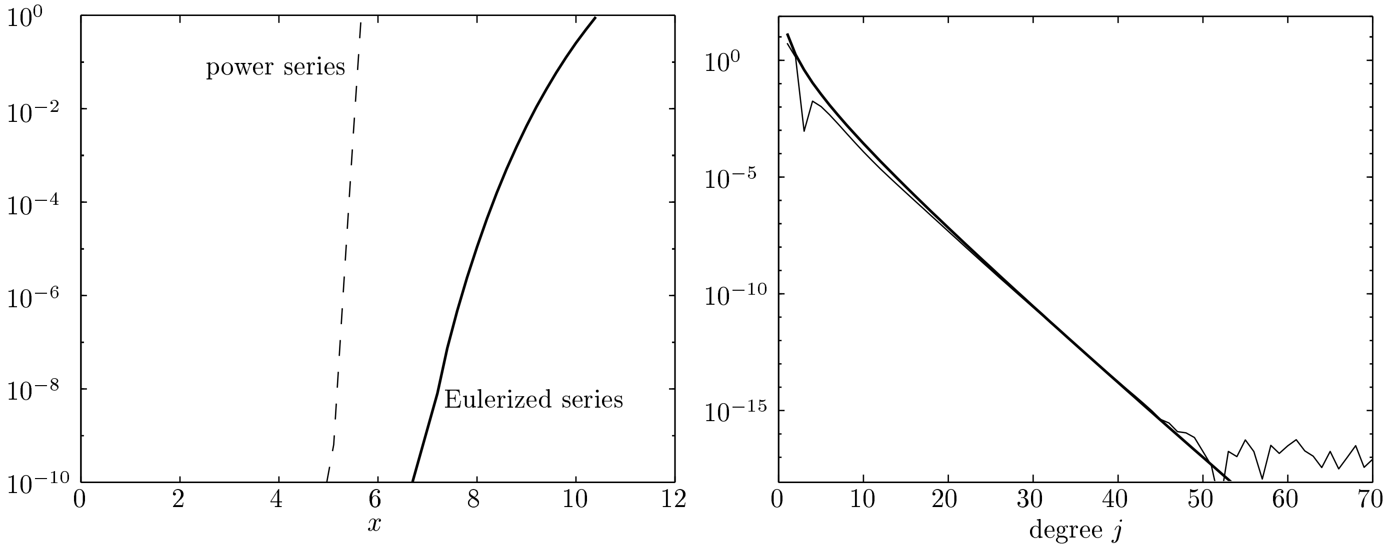

FIGURE 1. Left: errors in 50-term power series versus 50-term Eulerized series. Right: the numerically computed coefficients b_j of the Eulerized-power series (thin curve) are compared with the analytic fit to the coefficients, $b_j \sim (28/j^2)\, 2^{-j}$ (thick curve). The plateau in the thin curve is due to roundoff error.

where

$$y \equiv x/S$$

is a rescaled variable such that the convergence-limiting singularities are at $|y| = 1$. The a_j may be found through a simple recurrence relation given by Blasius [1908] or by the power series ODE-solver built into Maple. The Euler series is

$$f(y) = y^2 \sum_{j=1}^{\infty} b_j \, \zeta^{j-1},$$

where the Euler coefficients are calculated recursively by $b_1 = a_1$ and

$$b_m = \frac{1}{2^{m-1}} \sum_{p=1}^{m-1} a_{p+1} \frac{(m-2)!}{(p-1)! \, (m-1-p)!},$$

for $m = 2, 3, \ldots$.

The left panel of Figure 1 shows that the Eulerized series is accurate far beyond the radius of convergence ($|x| < 5.69$) of the ordinary power series.

Roundoff error makes it impossible in Matlab to compute accurate Euler coefficients (from those of the unaccelerated power series) for $j > 50$ as illustrated by the plateau in the upper right panel of Figure 1. Nevertheless, the accurately computed coefficients for $j \le 50$ fit rather well with

$$b_j \sim \frac{28}{j^2} \frac{1}{2^j}$$

as shown in the same graph. When power series coefficients decay as $1/\rho^j$, perhaps multiplied by algebraic factors of j such as j^{-2} here, the radius of convergence is ρ [Boyd 1989]. It follows that the Eulerized series, to the extent that the fit is credible, converges for $|\zeta| < 2$. The contours of constant $|\zeta|$ are equiconvergence contours for the Eulerized series in the sense that the expansion will converge at approximately the same rate for all x on such a contour. Figure 2 shows these contours. The series diverges in the shaded regions bounded by $\zeta = 2$, which are the images of the circle of convergence in the complex ζ-plane. It appears that the Eulerized series converges for all finite real positive x. The Eulerized series also tells us that the Blasius function is *free of singularities* in the unshaded regions where it converges; all the poles must lie somewhere in the three shaded domains.

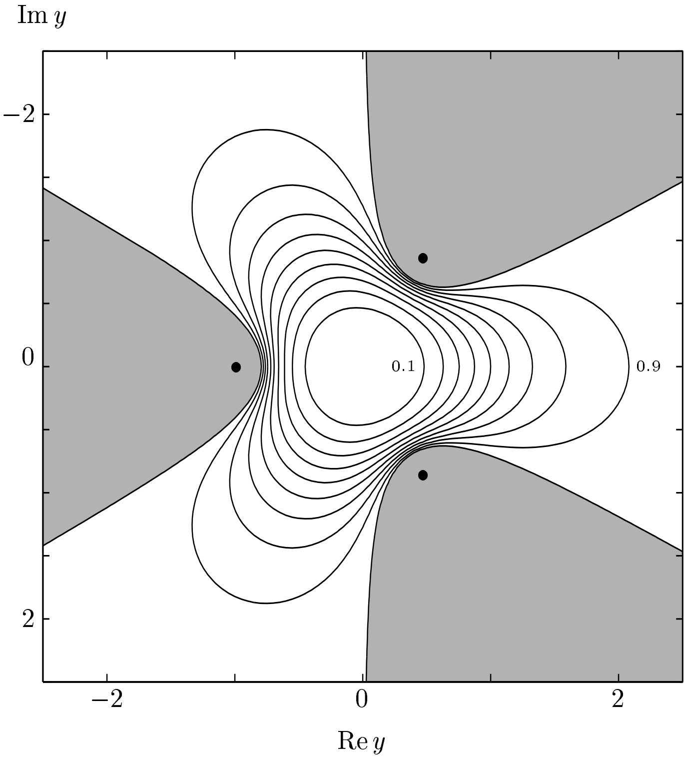

FIGURE 2. The magnitude of the j-th Euler term is roughly $|\zeta/2|^j$. Thus, by plotting contours of $|\zeta(y)/2|$, we can see curves in the complex y-plane (where $y = x/S$) where the series converges at a given rate. The shaded regions are where $|\zeta/2| > 1$, that is, are regions where the Eulerized series diverges. The dots show the three singularities that are nearest the origin.

5. PADÉ APPROXIMANTS

The article [Boyd 1997] showed how Padé approximants can be used to solve nonlinear boundary value problems. The $[m/n]$ approximant is the ratio of a polynomial of degree m divided by a polynomial of degree n which is formed from the power series through the algorithm described in [Baker 1965; 1975; Bender and Orszag 1978]. For the Blasius function, we divided f by x^2 and then approximated the remaining factor by a "diagonal" or $[N/N]$ approximant in the variable $w \equiv x^3$. This does not have the correct asymptotic behavior as $x \to \infty$. Nevertheless, for large but finite x, the approximant should converge, as the degree N tends to infinity, to the correct function. The unknown curvature κ is then adjusted for moderate x so that the approximant satisfies the asymptotic boundary condition $f_x = 1$.

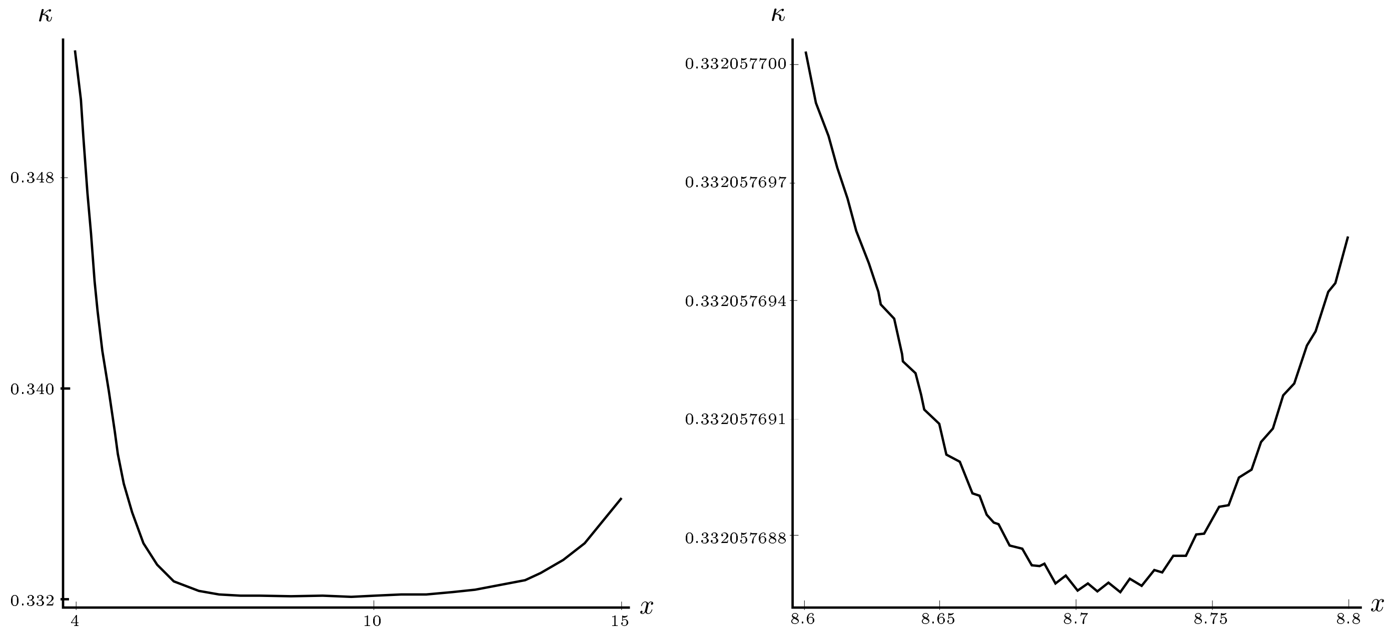

FIGURE 3. Zero contours of the boundary condition $f_x^{[10/10]}(x;\kappa) = 1$ as a function of x, the point where the condition is imposed, and κ, which is the value of $f_{xx}(0)$ used to solve the Blasius equation. $f^{[10/10]}$ is the Padé approximant to the Blasius function; this is x^2 times a polynomial of degree 10 in x^3 (that is, of degree 30 in x), divided by a different polynomial of the same degree.

In our previous work, we restricted $N \leq 8$ and displayed results only as a table generated by conventional root-finding. It is more illuminating to solve the problem graphically by drawing the zero contour of the boundary condition $f_x^{N,N}(x;\kappa) - 1$ as a function of x, the point where the boundary condition is imposed, and κ, which is the value of $f_{xx}(0)$ used in the power series (and Padé) approximations to f. Figure 3 illustrates this contour, for two different ranges in x, for the [10/10] approximant, which is derived from the power series up to and including x^{62}. The top graph was actually a plot for $\kappa \in [0, 1/2]$, but the Maple contour algorithm automatically restricted the axis limits to the much smaller range of κ spanned by the zero contour for $x \in [0, 15]$.

For small x, the slope of the true solution has not yet completely asymptoted to one, so the boundary condition $f_x = 1$ can be satisfied only by using values of the curvature which differ from that of the solution, and κ varies rapidly with x. For large x, the true solution does have a slope of one, but the Padé approximant is increasingly inaccurate as x increases. For intermediate x, both the asymptotic approximation $f_x \sim 1$ and the Padé approximation $f \approx f^{[10/10]}(x)$ are accurate, so the zero contour is flat, telling the truthful and consistent story that $\kappa \approx 0.332$.

The most accurate approximation is where the zero contour of the boundary condition varies least with x. The lower panel of Figure 3 shows that, on the zero contour, $\kappa(x)$ has a minimum for $x \approx 8.1$ for this order of approximant. The boundary condition $f_x^{[10/10]} = 1$ is satisfied at this x for $\kappa = 0.3320576856$. This approximation to κ has an absolute error of only 3.9×10^{-7}, which is a relative error of only 1 part in 8 million.

6. RATIONAL CHEBYSHEV NUMERICAL METHOD (TL SERIES)

The Eulerized power series is highly nonuniform in x in the sense that any finite truncation, such as the fifty terms illustrated in Figure 1, is exact at the origin and then deteriorates rapidly as x increases. This nonuniformity can be overcome by expanding the solution as a series of rational Chebyshev functions TL. These are simply the cosine functions of a Fourier series with a change of coordinate:

$$\mathrm{TL}_j(x;L) \equiv \cos(jt), \quad t(x) \equiv 2\,\mathrm{arccot}\,\sqrt{x/L}$$

The TL are rational functions of x.

The map parameter L is a constant which can be chosen to optimize the rate of convergence. After some experimentation, $L = 6$ proved best, but any choice between $L = 3$ and $L = 15$ was almost as good as the optimum.

All derivatives of these basis functions can be evaluated by applying the chain rule or the tables of [Boyd 1989; 1987]. The pseudospectral method is to substitute the expansion with undetermined coefficients into the problem and demand that the residual be zero at each of $N - b$ collocation points x_j where N is the number of terms in the series and b is the number of boundary conditions which must be explicitly applied. As explained in [Boyd 1989; 1987], the boundary condition of boundedness at infinity is a "natural" boundary condition, so $b = 2$ because only the boundary conditions at the origin need be imposed as explicit constraints. The result of these $N - 2$ collocation conditions plus the two boundary conditions give N algebraic equations in N unknowns which can be solved by Newton's iteration.

The only complication for the Blasius problem is that f is *not* bounded at infinity. However, if we make the split

$$f = x + v(x),$$

where

$$v(x) = \sum_{j=0}^{N-1} d_j \, \mathrm{TL}_j(x; L), \tag{6–1}$$

then the pseudospectral method can be applied as usual.

Figure 4 shows the convergence rate is remarkably fast; d_{100} is smaller than d_1 by roughly 10^{-14}! Table 3 on page 392 gives enough coefficients to evaluate f and its first three derivatives with an absolute error that is less than 10^{-9} over the whole real axis. A short Matlab implementation of this procedure is available upon request.

The theory of rational Chebyshev expansions (see [Boyd 1982]) predicts that the coefficients of a Gaussian function are asymptotically of the form

$$d_j = \{\} \exp\left(-1.199 j^{4/5}\right) \cos(3.2 j^{4/5} + \pi/6) \tag{6–2}$$

as obtained by substituting $L = 6$, $k = 2$, and $A = \frac{1}{4}$ in [Boyd 1982, Equations (3.16)–(3.18)], which describe the coefficients for the more general form $\exp(-Ax^k)$. The empty braces denote factors which vary more slowly with j than the functions which are explicitly displayed.

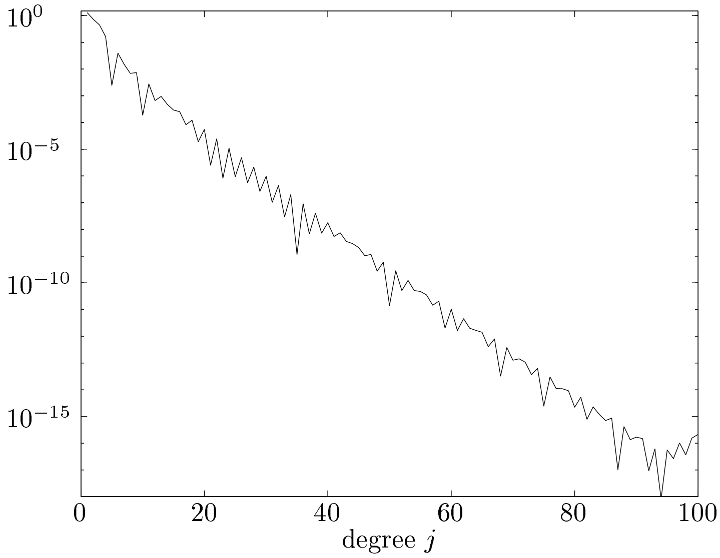

FIGURE 4. Absolute values $|d_j|$ of the coefficients of the rational Chebyshev functions of the Blasius function.

This asymptotic formula ignores the contributions of singularities of f which are enclosed within the steepest descent contour — the usual Fourier coefficient integral in the t-plane must be deformed from the real axis to pass through the complex-valued saddle point. However, for finite j, only a finite number of singularities is enclosed (although the number increases with j). Because, as explained later, $\arg x > \pi/4$ for all singularities of the Blasius function and the "saddle point" has $\arg(t) > \pi/10$, the images of all singularities within the steepest descent contour have $\mathrm{Im}\, t > \mathrm{Im}\, t_s$. This implies that their residues make contributions that are asymptotically negligible to that from the saddle point, yielding Equation (6–2).

The exponent r of the decay factor

$$\exp(-\text{constant } j^r)$$

is the "exponential index of convergence". It is defined as the limit (strictly speaking, an *infimum* limit) of

$$r_{\text{estimate}} \equiv \frac{\log\left|\log |d_j|\right|}{\log j}. \tag{6–3}$$

Figure 5 shows that even with these fluctuations embodied in the cosine factor in Equation (6–2), r_{estimate} appears to be converging to $r = \frac{4}{5}$ as it should. It is gratifying to see that the theoretical

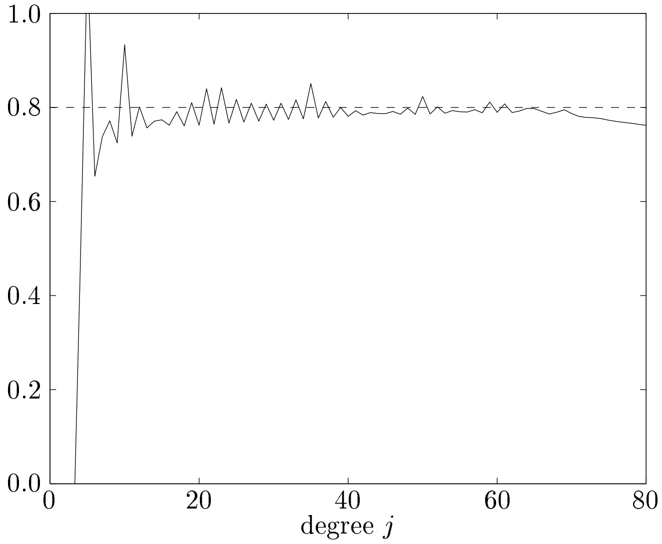

FIGURE 5. The estimate (6–3) for the exponential index of convergence r, versus the degree. The guideline is at $r = \frac{4}{5}$.

concept of an "exponential index of convergence" r can be verified for a nontrivial, engineering-relevant function.

For many problems with smooth, monotonic solutions, it is possible to obtain moderate accuracy with just one or two basis functions, allowing an *analytic* solution. Many examples are given in [Boyd 1989; Finlayson 1973] and in the article [Boyd 1993] on symbolic computer algebra and Chebyshev methods. The Blasius function is so smooth, and has such a tantalizing complex-plane symmetry, that it ought to be one of these functions that can be represented by a mere handful of functions — but it is not.

One needs at least seven TL to obtain the correct sign for the second derivative at the origin (Table 2). We made unsuccessful attempts to expand f as a function of x^2 times a TL basis in x^3, but were not able to find a good scheme. Perhaps the reader will be more ingenious!

7. STALKING THE WILD SINGULARITY

By substituting $f \sim R/x^\nu$ into the Blasius equation, one finds that the only possible choices for residue and exponent are those corresponding to the exact pole solution discussed earlier: $R = 6$ and $\nu = 1$. As the singularity is approached, the pole will more and more dominate the numerical values of f and its derivatives. To estimate the location of the singularity, we therefore calculated

N	$f_{xx}(0)$
6	-0.0148
7	0.2535
8	0.3426
10	0.3284
20	0.332213
40	0.3320572088

TABLE 2. Approximation of the second derivative at the origin (κ) by TL as a function of N ($L = 4$).

$$\sigma_1 \equiv x - 6/f(x), \quad \sigma_2 \equiv x - \sqrt{|-6/f_x|},$$
$$\sigma_3 = x - (|12/f_{xx}|)^{1/3},$$

while integrating away from the origin on the negative real x-axis. All three σ_j should converge to the location of the singularity as the pole is approached. By comparing these estimates, using an adaptive fourth- and fifth-order Runge–Kutta to apply a smaller and smaller step size as the pole is approached, we find the singularity is at $x = -S$, where $S \approx 5.6900380545$ and all digits shown are believed correct.

8. LOCAL ANALYSIS OF THE SINGULARITY: FIRST CORRECTION

To analyze the neighborhood of the singularity, it is convenient to define a new coordinate X:

$$X \equiv -\log(1 + x/S) \leftrightarrow x = S(e^{-X} - 1).$$

Note that $X = 0$ is equivalent to $x = 0$ while the singularity is moved to $X = \infty$.

The Blasius equation becomes

$$f_{XXX} + 3f_{XX} + 2f_X - \tfrac{1}{2}Se^{-X}(ff_{XX} + ff_X) = 0, \tag{8–1}$$

with initial conditions

$$f(0) = 0, \quad f_X(0) = 0, \quad f_{XX}(0) = S^2\kappa, \tag{8–2}$$

where $\kappa = 0.3320\ldots$.

The leading order approximation, a first order pole, becomes

$$f_{\text{pole}} = \frac{6}{S}e^X. \tag{8–3}$$

To calculate corrections, write $f = f_{\text{pole}} + p(X)$. The Blasius equation becomes

$$p_{XXX} - p_X - 6p = \tfrac{1}{2} S e^{-X} p(p_{XX} + p_X). \quad (8\text{–}4)$$

The linearization of this equation is

$$p_{1,XXX} - p_{1,X} - 6p_1 = 0, \quad (8\text{–}5)$$

where p_1 denotes the solution to this linearized equation. The advantage of the change-of-coordinate is now clear: Equation (8–5) is a *constant coefficient* equation and therefore may be solved analytically in terms of exponentials to give the general three-parameter solution

$$p_1 = \Lambda e^{2X} + A e^{-X} \cos(2^{1/2} X + \Phi).$$

The first term is more singular than f_{pole} — it is a second-order pole in the original coordinate — and is thus inconsistent with the linearization. Thus, $\Lambda = 0$ and the remaining challenge is to determine the amplitude A and phase Φ of the sinusoidal term.

The Blasius equation is unusual in that, because f_{pole} is an *exact* solution in its own right as well as the leading order approximation to the Blasius function, the linearized equation is *homogeneous*. (Linearization is employed in Newton's iteration, too, but the Newton–Kantorovich differential equation is almost always *inhomogeneous*.)

We determined A and Φ by curve-fitting the Blasius function f, as computed by Runge–Kutta integration in X of the full nonlinear differential equation. (One could of course integrate the linearized equation from $X = 0$, but the linearization is inaccurate at $X = 0$.) Although there is a certain ugliness in determining parameters by curve-fitting, Figure 6 shows that the fit to the first correction is quite good.

9. GENERALIZED STOKES EXPANSION: SECOND CORRECTION TO THE POLE

The second correction is obtained by substituting

$$f = \frac{6}{S} e^X + \frac{A}{2} e^{-X} \left(\exp(i 2^{1/2} + i\Phi) + \exp(-i 2^{1/2} - i\Phi) \right) + p_2(X) + \cdots$$

into the Blasius equation and neglecting quadratic terms in p_2 to obtain

$$p_{2,XXX} - p_{2,X} - 6p_2 = \tfrac{1}{2} S e^{-X} p_1 (p_{1,X} + p_{2,X}). \quad (9\text{–}1)$$

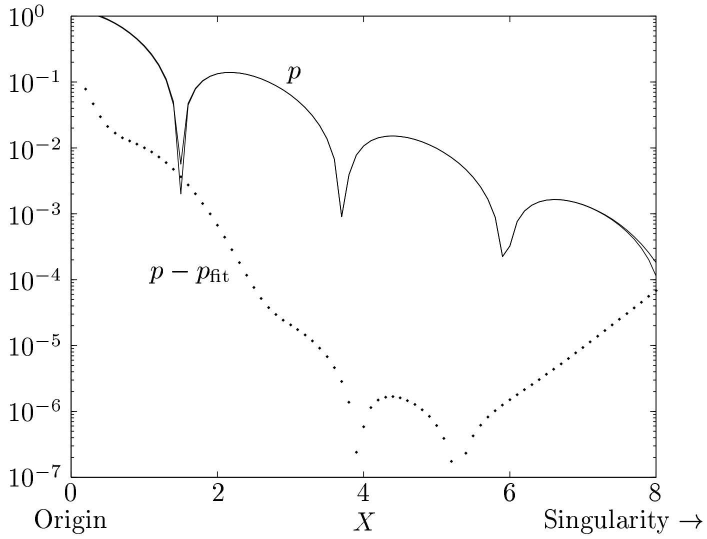

FIGURE 6. The two curves, which are almost indistinguishable, show the numerical solution p and the fitted approximation $p_{\text{fit}}(X) = f_{\text{pole}} - 1.5036 e^{-X} \times \cos(2^{1/2} X - 0.54454)$. The dots show the difference between the two, which is very small over most of the interval. The transformed variable X is defined in Section 8. The rise in error for $X > 5$ (where theoretically it should continue to decrease) is a numerical artifact.

Just as found by Stokes for water waves in 1847, the quadratic self-interaction of the sinusoidal function p_1 forces a second harmonic with twice the wavenumber. If we continue the perturbation theory to order j, the j-th order will contain a trigonometric function whose argument is proportional to $j\, 2^{1/2}$.

In particular, p_2 is given by

$$e^{-3X} \left(\beta_1 \cos(8^{1/2} X + 2\Phi) + \beta_2 \sin(8^{1/2} X + 2\Phi) + \beta_3 \right),$$

with

$$\beta_1 = -\tfrac{13}{1452} S A^2,$$
$$\beta_2 = -\tfrac{5}{2904} \sqrt{2} S A^2,$$
$$\beta_3 = \tfrac{1}{60} S A^2.$$

With our curve-fit values,

$$f_{\text{pole}} = 1.05447 e^X,$$
$$p_1 = -1.5036 e^{-X} \cos(2^{1/2} X - 0.54454),$$
$$p_2 = e^{-3X} \big(-0.1152 \cos(8^{1/2} X - 1.0891) - 0.021323 \sin(8^{1/2} X - 1.0891) + 0.2144 \big).$$

It is obvious that this process can be continued to any order, at least formally. One difference from the usual Stokes series described, with many historical references and illustrations, in [Boyd 1998; 1986, Haupt and Boyd 1988], is that higher terms are multiplied by powers of $\exp(-X)$ [$\propto y = x + S$]. The series converges geometrically fast near the singularity because of this.

In the original coordinate, the first correction is proportional to

$$\cos\left(\sqrt{2}\log(x+S) + \Phi'\right).$$

Thus, it oscillates an infinite number of times over a finite interval in x as the singularity is approached. To describe the singularity of the Blasius function as a "simple" pole is a serious abuse of common sense because the structure of the singularity is very complicated indeed, even though the leading order is merely a first order or "simple" pole.

Although the Stokes series appears to converge geometrically, there is no proof of convergence. We cannot as yet exclude the possibility of other terms, singular at $x = -S$ and decreasing faster than any finite power of $(x+S)$ as the singularity is approached. These would be transcendentally small ("beyond all orders") compared to the terms of the Stokes series and thus cannot be computed by the procedure described here, but rather require the heavier artillery of "exponential asymptotics" [Boyd 1998; 1999].

10. CARTOGRAPHY OF THE COMPLEX PLANE

To map the structure of the Blasius function in the complex plane, we integrated the differential equation for a large number of circular arcs , each begun on the real axis and continued to $\arg x = \pi/3$. The sector spanned by these arcs is only one-sixth of the complex plane. This is sufficient to map the whole plane for two reasons. First, f_{xx} has a power series in x^3 which implies a C_3-invariance in the complex plane. Each of the three sectors into which the plane is divided by the solid rays in Figure 7 is identical with the other two for f_{xx} and for $|f|$. (Because f itself is a function of x^3 multiplied by x^2, the values of f in the other two sectors are identical to those in right-hand sector except for multiplication by $\exp(i4\pi/3)$ or $\exp(i8\pi/3)$.) The second reason is that f is real-valued on the positive real axis. It follows that $|f|$ and $\operatorname{Re} f$ are symmetric with respect to the positive real axis, which is shown as a dotted line in the figure. Thus, mapping any one of the six sectors into which the complex plane is partitioned by the three solid and three dotted rays is sufficient to reconstruct the behavior in the other five portions of the plane. In the language of group theory, $|f|$ has a D_3 symmetry — invariant under rotations through any multiple of 120 degrees plus invariance with respect to reflections about an axis (the dotted rays in the figure) in the middle of each third of the plane.

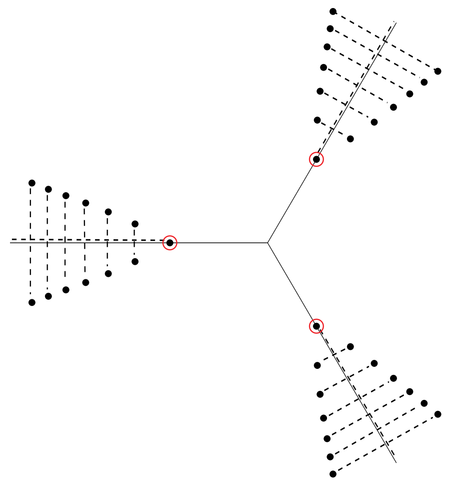

FIGURE 7. Schematic of the complex plane. The solid rays at $\arg x = \frac{1}{3}\pi, \pi, \frac{5}{3}\pi$ divide the plane into three sectors which are identical (for f_{xx} and $|f|$) if the branch cuts (dashed line segments) connecting the singularities (shown as black dots) are drawn in a symmetrical way. The choice of symmetry-consistent branch cuts is not unique; one particular choice is illustrated. Most of the singularities are connected in pairs by the branch cuts across the three solid dividing rays. The exceptions are the three unpaired singularities, shown as disks surround by circles, which are nearest the origin. The branch cuts from these are rays to infinity superposed on the heavy solid rays.

There are at least two choices of branch cuts which are consistent with D_3 symmetry. One such choice is illustrated in Figure 7. This choice is consistent with integrating the differential equation along the circular arcs $x = \rho \exp(i\theta)$, $\rho =$ constant, $\theta \in [0, \frac{\pi}{3}]$. The Runge–Kutta algorithm forces the numerical solution to be continuous and thus implicitly assumes that the path of integration is free of branch cuts.

A second choice, also consistent with symmetry, is to simply connect each singularity to $x = \infty$ by a

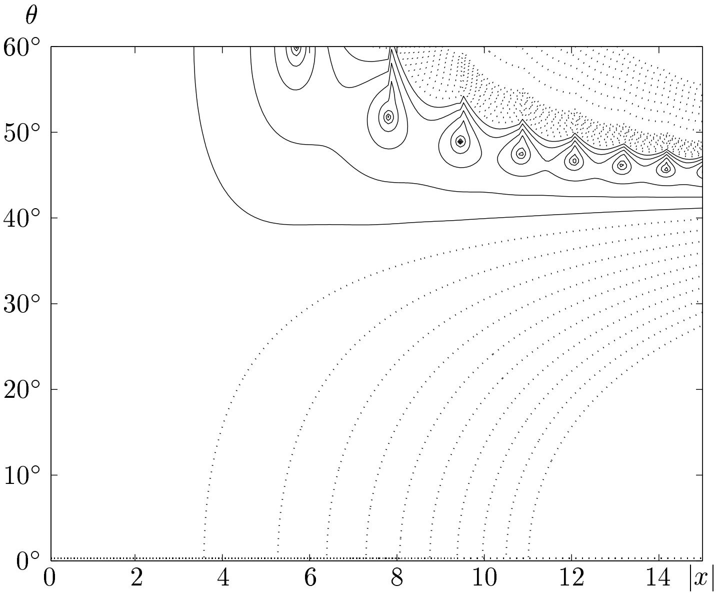

FIGURE 8. Contours of $\log_{10}|f_{xx}|$ in the complex plane as computed using circular arcs of integration, all begun from the real x-axis. Nonnegative contours are solid; negative contours are dashed. Contours have unit spacing except for the upper right corner where the contours for -20, -30, etc. are shown. 200 values of $|x|$ (200 arcs) were used with 5000 grid points for the fourth order Runge–Kutta integration. The bullseye-like clusters of circular contours denote the location of the singularities of f.

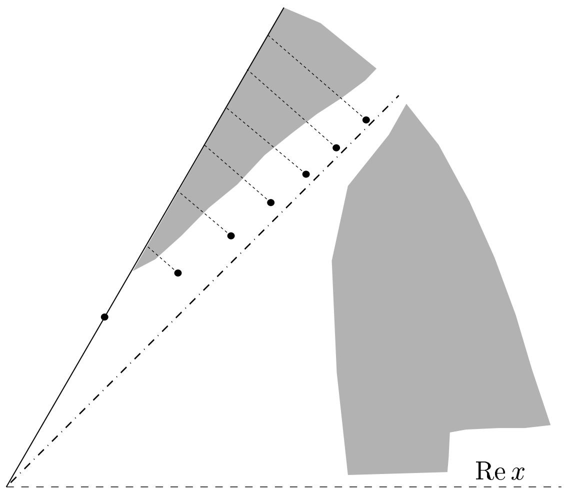

FIGURE 9. Schematic of a $\frac{\pi}{3}$ sector of the complex plane. The black dots indicate the singularities. The dash-dotted ray at $\arg x = \frac{\pi}{4}$ is the line where the real axis asymptotic approximation fails. We conjecture that the singularity locations asymptote to this ray as $|x|$ increases. The two shaded regions denote where the Blasius function f can be approximated by a *linear* polynomial (although the slopes are very different in the two regions.) The branch cuts are as illustrated in Figure 7; no circular arc from the real axis to $\arg x = \frac{\pi}{3}$ crosses a branch cut.

ray of constant θ where $\theta \equiv \arg x$. If we integrated the differential equation along radial paths from the origin, we would be implicitly adopting this choice of branch cut. Outside the region tesselated by these competing choices of branch cuts, the choice is irrelevant. We chose circular arcs because preliminary experiments showed that the integration was more stable (and needed few points) than mapping by radial integration paths.

Figure 8 shows, computing along a sequence of circular arcs, the numerical results, depicted through the contours of the *logarithm* of the absolute value of the curvature f_{xx} (rather than f itself). The negative contours of the logarithm (dashed) show where the curvature is very small and therefore where, at least for $|x| > 3$, f is well approximated by a linear function of x.

Blasius himself noted that, on the real axis,

$$f_{xx} = 0.234\exp\left(-\tfrac{1}{4}x\,(x - 3.44)\right) \quad \text{for } x \gg 1, \tag{10–1}$$

where the constants are given with greater precision in Equation (3–3) on page 383. The crucial point is that when we move off the real axis, the Gaussian function increases, but, for sufficiently large $|x|$, is still small compared to one everywhere within the sector $\arg x \in [-\frac{\pi}{4}, \frac{\pi}{4}]$. Since f itself is growing linearly with x, and the linear approximation to f is the justification for the Gaussian shape (and smallness) of f_{xx} as explained above (through solving $2f_{xxx} + ff_{xx} = 0$ as a first order ODE for f_{xx} under the assumption that $f \sim -1.72 + x$), it follows that (10–1) should be accurate everywhere within this sector, $\arg x \in [-\frac{\pi}{4}, \frac{\pi}{4}]$. Since the smallness of f_{xx} is obviously incompatible with a singularity, we conjecture on the basis of these asymptotics that f is free of singularities everywhere within $|\arg x| < \frac{\pi}{4}$.

Along the line $\arg x = \frac{\pi}{4}$, the curvature is as large as f itself, and the asymptotic analysis fails. Our numerical calculations show that the singularities seem to asymptote to this ray as $|x|$ increases. Indeed, the locations of the singularities can be connected to form a curve which is the center of a transition zone from the real axis asymptotics of Blasius to something else. The "something else" turns out be another region where f can be approximated by a linear polynomial, but with a much greater slope.

The linear family of exact solutions is an attractor in the sense that if $\operatorname{Re} f > 0$, then the Blasius equation itself shows that curvature satisfies

$$\frac{(f_{xx})_x}{f_{xx}} < 0, \qquad (10\text{–}2)$$

which forces the curvature f_{xx} to decay rapidly, in turn forcing f to asymptote to a linear polynomial. This creates the second region of negative, dashed contours of curvature in the upper right of Figure 8. Because the ray $\arg x = \frac{\pi}{3}$ is crossed by many branch cuts (with the choice of cuts appropriate for integration along circular arcs), the coefficients of the linear polynomial jump discontinuously at each cut.

Thus, the overall picture in a sector spanning sixty degrees in $\arg x$ is as depicted in Figure 9. Two separate regions of linear behavior are separated by a transition with singularities whose locations asymptote to a ray from the origin with $\arg x = \frac{\pi}{4}$.

11. CONJECTURES AND UNRESOLVED QUESTIONS

Our numerical experiments suggest:

Conjecture. *All singularities of the Blasius function lie within the radial sector $\theta \in [\pi/4, 5\pi/12]$ plus the two sectors obtained from this by rotation about the origin in the complex plane through angles of $2\pi/3$ and $4\pi/3$.*

If demonstrated, this conjecture would have the immediate corollary that the Euler-accelerated series would converge for all positive real x.

A second conjecture is that there is an infinite number of singularities and that the locations of these asymptotes to the ray $\arg x = \pi/4$ (and the five corresponding rays in other sectors) as $|x| \to \infty$.

The Blasius problem also poses some intriguing questions. First, given the rapid rate of convergence, why does one need at least 7 TL functions to obtain even a crude approximation? Why is it so hard to devise a good analytical approximation to a function which is monotonic and asymptotes rapidly to a linear polynomial?

Second, why are the singularities — poles plus an infinite series of logarithmic corrections — so complicated? Are there further corrections, perhaps proportional to $\exp(-\text{constant}/(x - x_s))$, which are transcendentally small compared to the cosine-of-log series discussed earlier?

Third, why does the physics of a boundary layer imply a C_3 symmetry in the complex plane, and an infinite pattern of pole-plus-cosine-of-logarithm singularities confined to narrow sectors?

The Blasius function is also noticeable for what it does not display. The locations of the singularities to many famous nonlinear ordinary differential equations such as the Lorenz system and the Duffing oscillator form very complicated patterns with a fractal structure. These fractal curves may be natural boundaries beyond which the function has no analytic continuation [Chang et al. 1982; 1983; Tabor and Weiss 1981; Fournier et al. 1988]. In marked contrast, the singularities of the Blasius function appear to be isolated and discrete. However, a rigorous

j	d_j		j	d_j		j	d_j		j	d_j		j	d_j	
1	−1.29633007174967		17	8.240572232304953	−5	33	−2.922628101455539	−8	49	5.948997	−10	65	−1.4191937	−12
2	−0.73007371589937		18	−1.211900272178847	−4	34	−1.999133757410387	−7	50	−1.425204994	−11	66	4.0957628	−13
3	0.44808018757846		19	−1.915852492525586	−5	35	1.1621141526	−9	51	−2.840214	−10	67	8.0169682	−13
4	−0.16361350641264		20	5.508949359351957	−5	36	9.081089641299	−8	52	−5.152015	−11	68	3.2677971	−14
5	−2.441619336720839	−3	21	2.522961313480479	−6	37	6.8351176675038	−9	53	1.240789	−10	69	−3.7832863	−13
6	3.965162549838397	−2	22	−2.449871878116695	−5	38	−4.073599849	−8	54	5.145303	−11	70	−1.2835719	−13
7	−1.498314265405804	−2	23	8.256052721985555	−7	39	−7.234976345	−9	55	−4.77717	−11	71	1.4452443	−13
8	−6.899795433728594	−3	24	1.082435361567464	−5	40	1.7831397	−8	56	−3.549064	−11	72	1.0664167	−13
9	7.354027000875889	−3	25	−9.467824259183999	−7	41	5.45995274	−9	57	1.4604904	−11	73	−3.686789	−14
10	1.883816492482166	−4	26	−4.795937231672587	−6	42	−7.4912183978	−9	58	2.0504416	−11	74	−6.346098	−14
11	−2.792174323932853	−3	27	5.628131255177790	−7	43	−3.553380147	−9	59	−2.022446	−12	75	−2.449579	−15
12	6.587260808050913	−4	28	2.141686005620873	−6	44	2.9417093785	−9	60	−1.036076	−11	76	3.010344	−14
13	9.475077735890138	−4	29	−2.646166147226868	−7	45	2.10524715	−9	61	−1.6526330	−12	77	1.115762	−14
14	−4.761820769583224	−4	30	−9.654176751560853	−7	46	−1.0248602	−9	62	4.5632488	−12	78	−1.093124	−14
15	−2.945676766131983	−4	31	1.026610305863982	−7	47	−1.15822758	−9	63	1.9982020	−12	79	−9.14531	−15
16	2.537311676664253	−4	32	4.385787776046917	−7	48	2.73175919	−10	64	−1.6650512	−12	80	2.21472	−15

TABLE 3. The first 80 coefficients of the TL series (6–1), given as mantissa and exponent (so $d_{80} = 2.21472 \times 10^{-15}$).

proof is lacking; with numerical experiments, we can only hope to explore part of the complex plane.

The Blasius function also teaches some lessons: with tricks, both Euler acceleration and rational Chebyshev expansion are very successful here. The difficulty with the Euler method is that f is the product of x^2 with a function of x^3; the trick is to modify the usual Euler change of coordinate by making it a function of x^3 after first extracting the x^2 factor. The complication for the Chebyshev series is that f is unbounded, but after writing $f = x + v(x)$, the bounded function v can be expanded as a TL series without complications; 80 terms give an absolute error less than 10^{-9}.

This work was motivated primarily by pure curiosity. For physical applications, a graph of f on the positive real axis of only moderate accuracy is probably sufficient. Nevertheless, there are practical lessons in the singularity analysis and complex-plane cartography, too. The smoothness and monotonicity for real x belie a complex-plane structure which is rather complicated. No nonlinear differential equation relevant to engineering, it seems, is too simple to be uncomplicated off the real axis.

ACKNOWLEDGEMENTS

I thank the reviewers for helpful comments.

REFERENCES

[Bairstow 1925] L. Bairstow, *J. Royal Aeronautical Soc.* **19** (1925), 3.

[Baker 1965] G. A. Baker, Jr., "Padé Approximants", pp. 1–50 in *Advances in Theoretical Physics*, vol. 1, Academic Press, New York, 1965.

[Baker, Jr. 1975] G. A. Baker, Jr., *Essentials of Padé Approximants*, Academic Press, New York, 1975.

[Bender and Orszag 1978] C. M. Bender and S. A. Orszag, *Advanced Mathematical Methods for Scientists and Engineers*, McGraw-Hill, New York, 1978.

[Blasius 1908] H. Blasius, "Grenzschichten in Flüssigkeiten mit kleiner Reibung", *Zeitschrift fur Mathematik und Physik* **56** (1908), 1–37.

[Boyd 1982] J. P. Boyd, "The optimization of convergence for Chebyshev polynomial methods in an unbounded domain", *Journal of Computational Physics* **45** (1982), 43–79.

[Boyd 1986] J. P. Boyd, "Solitons from sine waves: analytical and numerical methods for non-integrable solitary and cnoidal waves", *Physica D* **21** (1986), 227–246.

[Boyd 1987] J. P. Boyd, "Orthogonal rational functions on a semi-infinite interval", *Journal of Computational Physics* **70** (1987), 63–88.

[Boyd 1989] J. P. Boyd, *Chebyshev and Fourier spectral methods*, Springer, New York, 1989.

[Boyd 1993] J. P. Boyd, "Chebyshev and Legendre spectral methods in algebraic manipulation languages", *J. Symb. Comput.* **16** (1993), 377–399.

[Boyd 1997] J. P. Boyd, "Padé approximant algorithm for solving nonlinear ODE boundary value problems on an unbounded domain", *Computers and Physics* **11**:3 (1997), 299–303.

[Boyd 1998] J. P. Boyd, *Weakly nonlocal solitary waves and other exponentially small phenomena*, Kluwer, Amsterdam, 1998.

[Boyd 1999] J. P. Boyd, "The devil's invention: asymptotics, superasymptotics and hyperasymptotics", *Acta Applicandae* **56** (1999), 1–98.

[Chang et al. 1982] Y. F. Chang, M. Tabor, and J. Weiss, "Analytic structure of the Hénon–Heiles Hamiltonian in integrable and nonintegrable regimes", *J. Math. Phys.* **23**:4 (1982), 531–538.

[Chang et al. 1983] Y. F. Chang, J. M. Greene, M. Tabor, and J. Weiss, "The analytic structure of dynamical systems and self-similar natural boundaries", *Phys. D* **8**:1-2 (1983), 183–207.

[Drazin and Tourigny 1996] P. G. Drazin and Y. Tourigny, "Numerical study of bifurcations by analytic continuation of a function defined by a power series", *SIAM J. Appl. Math.* **56**:1 (1996), 1–18.

[Finlayson 1973] B. A. Finlayson, *The method of weighted residuals and variational principles*, Academic Press, New York, 1973.

[Fournier et al. 1988] J.-D. Fournier, G. Levine, and M. Tabor, "Singularity clustering in the Duffing oscillator", *J. Phys. A* **21**:1 (1988), 33–54.

[Haupt and Boyd 1988] S. E. Haupt and J. P. Boyd, "Modeling nonlinear resonance: a modification to Stokes' perturbation expansion", *Wave Motion* **10** (1988), 83–98.

[Hunter and Lee 1986] C. Hunter and S. M. Lee, "The analytic structure of Oseen flow past a sphere as a function of Reynolds number", *SIAM J. Appl. Math.* **46**:6 (1986), 978–999.

[Hunter and Tajdari 1990] C. Hunter and M. Tajdari, "Singular complex periodic solutions of Van der Pol's equation", *SIAM J. Appl. Math.* **50**:6 (1990), 1764–1779.

[Meiron et al. 1982] D. I. Meiron, G. R. Baker, and S. A. Orszag, "Analytic structure of vortex sheet dynamics, 1: Kelvin–Helmholtz instability", *J. Fluid Mech.* **114** (1982), 283–298.

[Meksyn 1956] D. Meksyn, "Integration of the boundary-layer equations", *Proc. R. Soc. A* **237** (1956), 543–559.

[Meksyn 1959] D. Meksyn, *C. R. Acad. Sci. Paris* **248**:16 (1959), 2286.

[Meksyn 1961] D. Meksyn, *New methods in laminar boundary-layer theory*, Pergamon Press, New York, 1961.

[Ostrowski 1948] A. Ostrowski, "Sur le rayon de convergence de la série de Blasius", *C. R. Acad. Sci. Paris* **227** (1948), 580–582.

[Piercy and Preston 1936] N. A. V. Piercy and J. H. Preston, *Philosophical Magazine* **21**:7 (1936), 995.

[Punnis 1956a] B. Punnis, "Zur Differentialgleichung der Plattengrenzschicht von Blasius", *Zeitschrift für Angewandte Mathematik und Mechanik* **36** (1956), S26.

[Punnis 1956b] B. Punnis, "Zur Differentialgleichung der Plattengrenzschicht von Blasius", *Arch. Math.* **7** (1956), 165–171.

[Squire 1959a] W. Squire, "Application of generalized Gauss-Laguerre quadrature to boundary-layer problems", *J. AeroSpace Sci.* **26** (1959), 540–541.

[Squire 1959b] W. Squire, "A note on the Blasius equation with three-point boundary conditions", *J. AeroSpace Sci.* **26** (1959), 678–679.

[Tabor and Weiss 1981] M. Tabor and J. Weiss, "Analytic structure of the Lorenz system", *Phys. Rev. A* **24** (1981), 2157–.

[Töpfer 1912] K. Töpfer, "Bemerkung zu dem Aufsatz von H. Blasius 'Grenzschichten in Flüssigkeiten mit kleiner Reibung'", *Zeitschrift für Mathematik und Physik* **60** (1912), 397–398.

[Treve 1967] Y. M. Treve, "On a class of solutions of the Blasius equation with applications", *SIAM J. Appl. Math.* **15** (1967), 1209–1227.

[Van Dyke 1974] M. Van Dyke, "Analysis and improvement of perturbation series", *Quart. J. Mech. Appl. Math.* **27** (1974), 423–449.

[Van Dyke 1975a] M. Van Dyke, "Computer extension of perturbation series in fluid mechanics", *SIAM J. Appl. Math.* **28**:3 (1975), 720–734.

[Van Dyke 1975b] M. Van Dyke, *Perturbation methods in fluid mechanics*, 2d ed., Parabolic Press, Stanford, CA, 1975.

[Van Dyke 1977] M. Van Dyke, "From zero to infinite Reynolds number by computer extension of Stokes series", *Lecture Notes in Math., Springer* **594** (1977), 506–517.

[Van Dyke 1978] M. Van Dyke, "Extended Stokes series: laminar flow through a loosely coiled pipe", *J. Fluid Mech.* **86** (1978), 129–145.

[Van Dyke 1984] M. Van Dyke, "Computer-extended series", *Ann. Rev. Fluid Mech.* **16** (1984), 287–309.

[Van Dyke 1990] M. Van Dyke, "Fluid mechanics off the real axis", pp. 355–366 in *Engineering Science and Fluid Dynamics*, edited by G. T. Yates, World Scientific Publishing, Singapore, 1990.

[Weyl 1941] H. Weyl, "Concerning the differential equations of some boundary layer problems", *Proc. Natl. Acad. Sci. USA* **27** (1941), 578–583.

[Weyl 1942a] H. Weyl, "Concerning the differential equations of some boundary layer problems, II", *Proc. Natl. Acad. Sci. USA* **28** (1942), 100–101.

[Weyl 1942b] H. Weyl, "On the differential equations of the simplest boundary-layer problems", *Ann. Math.* **43** (1942), 381–407.

John P. Boyd, Department of Atmospheric, Oceanic and Space Science and Laboratory for Scientific Computation, University of Michigan, 2455 Hayward Avenue, Ann Arbor MI 48109, United States (jpboyd@umich.edu, http://www.engin.umich.edu:/~jpboyd/)

Received November 6, 1997; accepted in revised form November 5, 1998